IJ**BMS**

An *in situ* forming gelatin-based hydrogel loaded with soluble amniotic membrane promotes full-thickness wound regeneration in rats

Mohammad Azimi-Alamouty [1,2], Mohammad amin Habibi [3], Amin Ebrahimi Sadrabadi [2], Zahra Jamalpoor [1]*

[1] Trauma Research Center, Aja University of Medical Sciences, Tehran, Iran
[2] Department of Tissue Engineering, Faculty of Basic Sciences and Advanced Technologies in Medicine, Royan Institute, ACECR, Tehran, Iran
[3] Iranian Tissue Bank and Research Center, Gene, Cell and Tissue Institute, Tehran university of Medical Sciences, Tehran, Iran

A B S T R A C T

Objective(s): Early effective treatment and appropriate coverage are vital for full-thickness wounds. Amnion membrane-derived products have recently emerged in tissue engineering. However, the optimal concentration, carrier for controlled release, and handling have remained challenges. This study aims to develop and optimize an *in situ* forming, amniotic-based hydrogel for wound healing.
Materials and Methods: Here, a composite matrix was fabricated with gelatin hydrogel modified with methacrylate functional group conjugated (GelMA) and keratose (wt.1%), loaded with mesenchymal stem cells (MSCs, 1×10^5 cell/ml) and optimized soluble amniotic membrane (SAM, 0.5 mg/ml). The physicochemical properties of the final subject were evaluated *in vitro* and *in vivo* environments.
Results: The results of the *in vitro* assay demonstrated that conjugation of the methacryloyl group with gelatin resulted in the formation of GelMA hydrogel (26.7 ± 1.2 kPa) with higher mechanical stability. Modification of GelMA with a glycosaminoglycan sulfate (Keratose) increased controlled delivery of SAM (47.3% vs. 84.3%). Metabolic activity (93%) and proliferation (21.2 ± 1.5 µg/ml) of MSCs encapsulated in hydrogel improved by incorporation of SAM (0.5 mg/ml). Furthermore, the migration of fibroblasts was facilitated in the scratched assay by SAM (0.5 mg/ml)/MSCs (1×10^5 cell/ml) conditioned medium. The GelMA hydrogel groupes revealed regeneration of full-thickness skin defects in rats after 3 weeks due to the high angiogenesis (6.3 ± 0.3), cell migration, and epithelialization.
Conclusion: The results indicated in situ forming and tunable GelMA hydrogels containing SAM and MSCs could be used as efficient substrates for full-thickness wound regeneration.

▶ Please cite this article as:
Azimi-Alamouty M, Habibi MA, Ebrahimi Sadrabadi A, Jamalpoor Z. An *in situ* forming gelatin-based hydrogel loaded with soluble amniotic membrane promotes full-thickness wound regeneration in rats. Iran J Basic Med Sci 2024; 27: 1005-1014. doi: https://dx.doi.org/10.22038/IJBMS.2024.74290.16140

Introduction

Wound healing is a complex and vital process that requires effective treatment and timely coverage to ensure optimal functional outcomes, especially in full-thickness and extensive wounds (1–3). Skin tissue has self-regenerated properties, and endogenous repair begins immediately after damage (4). Platelet accumulation initiates the coagulation phase, which is followed by the migration of immune cells into the wound area, where they work with growth factors to remove germs and foreign bodies (5, 6). In the proliferation phase, fibroblasts and keratinocytes become engaged, resulting in tissue formation and epithelialization. Several intricate activities are occurring during this dynamic time, including the development of extracellular matrix (ECM), the production of soluble mediators, parenchymal cell proliferation, and migration (6, 7). However, increased immune cells, cell apoptosis, and growth factor distraction may cause the normal healing process to be interrupted or delayed in individuals with full-thickness wounds (8, 9). With the development of tissue engineering products, Advanced Therapeutic Medicinal products (ATMPs) have

demonstrated success in skin tissue regeneration (10, 11). Additionally, cell-based and biological products enhanced the transfer of exogenous cells and molecules to the wound site and produced a proper and moist environment for the proliferation and migration of the native cells (10, 11). The viability of the encapsulated cells in the carrier, the type of carrier (12), mechanical and biological properties, and the choice of biomolecules and cytokines (13) for delivery to the wound site are still the main challenges and drawbacks of skin substitutes, and various studies have been conducted on this subject matter. In the early stages of tissue repair, cell-to-cell communication was regulated by growth factors (8). Proteomics analysis of amniotic membrane (AM) revealed a large range of growth factors, cytokines, proteases, soluble receptors, and other proteins (14, 15). The application of amniotic membrane was limited in the undermined, cavity, and deformed wounds (16, 17). A soluble form of AM has been shown to repair ocular damage and wounds today (16, 18). Indeed, according to AME proteomics analysis, a number of therapeutic growth factors have been approved for use in tissue regeneration (18–20). As tissue

Corresponding author: Zahra Jamalpoor. Trauma Research Center, Aja University of Medical Sciences, Tehran, Iran, West Fatemi St, Etemad Zadeh St. Aja University of Medical Sciences, Tehran, Iran. Email: z_jamalpoor2000@yahoo.com, z.jamlapoor@ajaums.ac.ir

regeneration is a complex process and numerous elements were involved (19), we prepared a cocktail of soluble proteins derived from amniotic membranes. Exogenous signals are released by various growth factor panels in response to changes in their local environment (15). The solubilized amnion membrane's total protein content may be quantified, and the optimum concentration in addition to the combination of SAM and cells in the fabrication of biological dressing can be assessed and optimized. Various hydrogel biomaterials have been recently investigated for applications in regenerative medicine, including as delivery systems for medications (21), proteins (22), and living cells (23). Natural hydrogels with minimal antigenicity, excellent biocompatibility, biodegradability, and affordability, like gelatin (i.e., hydrolyzed collagen), have gained increased popularity (24). Gelatin's mechanical properties were improved when it was modified with methacrylate functional groups conjugated onto the amine or hydroxyl groups (25, 26). Affinity of hydrogel was further improved by the sulfated group (27, 28). Keratose, the oxidized form of keratin, may be appropriate for affinity-based drug delivery systems due to the presence of sulfonate functional groups (29). Most membrane and film dressings on the market are difficult to apply, so in situ formed dressings are preferable to self-prefabricated (30). In situ forming hydrogels that could contour wound defects have an advantage over the use of prefabricated hydrogel scaffolds as they would allow the dressing to conform to the wound without folding or nicking (31). A combination of tissue engineering and cell-based therapies is a promising approach for full-thickness wound healing (32). MSCs can produce biological factors modulating the immune response, proliferation, migration of keratinocyte and endothelial cells, and invocation of macrophages and endothelial progenitor cells to the wound area and cause angiogenesis (33). This study aims to develop and optimize an in situ forming, soluble amniotic membrane (SAM)-loaded cell-based hydrogel to promote full-thickness wound regeneration in rats.

Materials and Methods
Materials
Lyophilized powdered gelatin from porcine skin (Type A, 9000-70-8), Dulbecco's minimal essential medium (DMEM), Ham's F12 medium (DMEM/F12,1:1), methacrylate anhydride (MA,760-93-0), penicillin/streptomycin, amphotericin B, fetal bovine serum (FBS), dimethyl sulfoxide (DMSO), hydrochloric acid (HCl), collagenase type II (17101015), 2-hydroxy-4'-(2-hydroxyethoxy)-2-methylpropiophenone (Irgacure 2959, Sigma 106797-53-9), 3-(4,5-dimethylthiazol-2-yl)-2,5-diphenyltetrazolium bromide (MTT reagent) and Trypan blue were purchased from Sigma-Aldrich (Dayaexir Co, Iran). The dehydrated amniotic membrane was supplied by Pishtaz Tebbe Abadis Co (Iran). keratose (KOS) was provided by Zharf Andishan Fanavar Zist Bespar Co (Iran). MTT and MTS Assay Kit (Cell Proliferation, Colorimetric) (ab197010) and Mouse/Rat Anti-CD31 antibody (ab28364) were purchased from Abcam.

Preparation of in situ forming cell-based SAM-loaded hydrogel
Synthesis of gelatin methacrylamide (GelMA)
Porcine skin gelatin powder (Type A, 10% w/v) was dissolved in Dulbecco's phosphate-buffered saline (DPBS) with stirring at 60 °C. Then, methacrylic anhydride (MA, 8.0 ml) was added to react with the gelatin solution with vigorous stirring at 50 °C for 3 hr. The reaction was stopped by diluting the polymer solution five-fold with hot DPBS (40 °C). The salts and unreacted MA were removed from the mixture by dialysis with a cut-off of 12-14 kDa in distilled water at 40 °C for 72 hr. White porous foam was then obtained by lyophilizing the solution for 48 hr and stored at -80 °C (34).

Preparation of soluble amniotic membrane
The dehydrated amniotic membrane (DAM) was cut into small pieces, and soft powder was obtained by grinding frozen DAM with a miller machine. DAM powder (10% w/v) was dispersed in PBS (100 ml) and the pepsin enzyme (1% w/v) and HCl (0.01 mol/l) were added to the resultant solution, and then incubated for 48 hr at 4 °C. The DAM solution was neutralized with Sodium Hydroxide (5 mol/l) and centrifuged (18000 rpm) for 5 min. Subsequently, the supernatant was removed and proteins were stable by protease inhibitor (PI; 0.1% w/v). The solution was called solubilized AM (SAM) and was sterilized by filtering (0.2 μm) and kept at -80 °C (15).

Fabrication of in situ forming cell-based SAM-loaded hydrogel
GelMA lyophilized powder (10% w/v) was sterilized by gamma-ray irradiation (25 Gy). Subsequently, the sterile powder was dissolved in DPBS containing 0.5% w/v 2-hydroxy-1-4- (hydroxyethyl) phenyl) -2-methyl-1-propanone (Irgacure 2959); as a photoinitiator at 80 °C to reach final GelMA concentrations at 10% w/v. Furthermore, the SAM solution was diluted with DPBS (0.1, 0.5, 1, and 1.5 mg/ml), and the concentration was then optimized. For this aim, the ucMSCs (Pasteur Institute of Iran) were cultured to fourth passage, followed by short trypsinization, isolated cells (1×10^5 cells/ml) responded with SAM solution (0.5 mg/ml) and were added to GelMA prepolymer solution (Figure 1). The resultant solution was poured into the wound site with a 27-gauge syringe, instantly exposed to UV light (360–480 nm) for 60 sec.

Characterization of physical properties of GelMA hydrogels
FTIR analysis and determination of the crosslinked Component of GelMA
GelMA and NpGel hydrogel were dried and materials
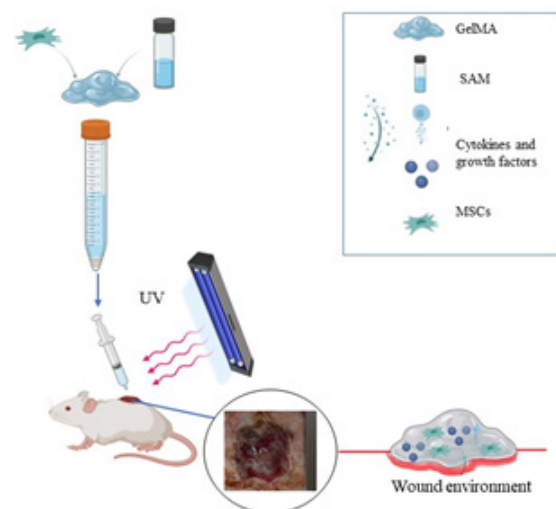
Figure 1. Fabrication SAM-loaded cell-laden hydrogel steps
MSCs and SAM loaded in GelMA hydrogel. Prepolymer hydrogel was poured in situ on the wound created on the back of the rat
SAM: Solubilized amniotic membrane

were ground and subject to Fourier transform infrared spectrometry assessed at a resolution range of 400–4000 cm⁻¹. Samples (10 mm diameter, 3 mm thickness) were fabricated upon UV (360-480) exposures for compression, swelling ratio, and degradation assessment. Non-photo-crosslinking Gelatin (NpGel) hydrogel was obtained as a control sample. GelMA and NpGel hydrogel was lyophilized for 48 hr and then the dry weight of the hydrogels was recorded (w_0). Hydrogels were immersed in HCL) 10 mM, pH: 2) for 24 hr at 4 °C. Rehydrated hydrogel scaffolds were lyophilized again and the dry weights were recorded (w). This manner (35) was repeated three times, non-reacted soluble gel and residual weight was calculated as follows:

Remaining weight (%) $=[(w_0-w)/w_0 \times 100]$

Compressive mechanical analysis

Photo-crosslinked hydrogel samples fabricated with or without cells or SAM, un-crosslinked were evaluated in terms of compressive mechanical properties with tested using a uniaxial compression, a universal electromechanical testing machine (Santam, STM-20, 60 N load cell) at a crosshead speed of 1 mm.min−1. The compressive modulus was calculated as the slope of the stress–strain curve at 10% strain.

Biodegradation rate

The degradation profile of hydrogels was assessed by incubation of hydrogel samples (d_0) in the enzymatic environment. To this aim, hydrogels were soaked in Eppendorf tubes (1.5 ml) containing DPBS with type II collagenase (2 U ml-1) for 3 weeks, which adjusted to the collagenase concentration during wound healing (36). In order to maintain constant enzyme activity, the collagenase solution was refreshed every three days. At predetermined intervals, samples were washed with sterilized deionized water twice, freeze-dried, and their dry weight measured.

Degradation rate (%) $=[(d_0-d)/d_0 \times 100]$

Swelling ratio analysis

Hydrogels were soaked in DPBS (pH: 7.4) at 37 °C for 24 hr. The filter paper was used to wipe off the excess water, and swollen weights of samples were recorded (s). The swelling ratio of the swollen gel was calculated according to the equation:

Swelling ratio (%) $=[(S_0-S)/S_0 \times 100]$

In vitro protein release assay

SAM (0.5 mg/ml) was mixed with the hydrogels (GelMA 10% w/v, KOS 1% w/v). The SAM-loaded hydrogels were immersed in a buffer solution containing PBS for 7 days. 1, 3, 7, and 14 days were chosen as the test time intervals. The supernatants were removed and new buffer added at each interval. According to the manufacturer's instructions, the manufacturer's ELISA kit (R&D Systems) was used to measure the release of epidermal growth factor (EGF) from the SAM-loaded in the hydrogel. The following equation was used to determine the percentage of release:

Release (%) = amount of released EGF/ amount of total EGF in SAM

Evaluation of cell viability in SAM-loaded hydrogel

Different concentrations of SAM (0.1, 0.5, 1, and 1.5 mg/ml) were loaded within MSCs-laden hydrogel. Cell viability,

proliferation, and efficacy of condition medium released from cell-laden hydrogel were assessed.

MTS assay

According to the manufacturer's instructions, the MTS assay was used to measure the metabolic activity of the MSCs loaded within the hydrogels. Cells bioreduce the MTS chemical into a colorful formazan product that is soluble in the media used for cell culture. It is assumed that the NADPH or NADH produced by the dehydrogenase enzymes in metabolically active cells will be used for this conversion. The number of live cells in the culture directly relates to the amount of formazan product. The cells/hydrogel were rinsed with PBS after specified incubation intervals of 1, 3, and 7 days. The media was then changed to MTS solution (1:5 dilution in culture medium), which was then incubated in the dark for 3 hr at 37 °C and 5% $CO2$. The optical density (OD) was measured at 490 nm in an ELISA plate reader.

Quantification of DNA content

In order to assess cell proliferation within the hydrogels, the total DNA content was evaluated. On day 14 of the culture, the cell-laden hydrogels had been totally homogenized and dissolved. The samples were processed with proteinase K (10 mg/ml) and lysis buffer (50 mmol/L tris-HCl, 50 mmol/L EDTA, 1 wt.% SDS, 10 mmol/L NaCl, pH 8.0) overnight at 65 °C. Then, using phenol/chloroform extraction and EtOH precipitation, DNA was removed from the aqueous phase. The resulting pellet was dissolved in water free of RNase, and we used a spectrophotometer to measure the amount of DNA at 280 nm. In terms of dry weight, the DNA concentration was given as g/mg of hydrogel.

Percentage of living cells = Average uptake of treated samples / Average uptake of control samples×100

Effect of CM on fibroblast migration

The conditioned medium prepared was assessed for in vitro wound healing. Briefly, human dermal fibroblasts (25 × 10⁴ cells/well) were cultured on 6-well plates, after they achieved 80% confluency, they were scratched with a pipette tip along a straight line. After washing the cell debris with PBS, HDFs were treated with CM and a CM-free serum-free culture media as a negative control. A completed culture media (DMEM/FBS 10%) was supplied to the positive control. Digital pictures of the cells were acquired using an Olympus device at 0, 6, 12, and 24 hr after scratching. Image-J software was then used to evaluate the pictures. A vertical line was drawn to mark each well below the surface of the screen. The percentage of scratch closure was calculated as follows = $[(S_0-S)/S_0] \times 100$, where S_0 is the scratch area at time 0 and at is the scratch area at 6, 12, and 24 hr.

In vivo wound healing study

The Ethics Committee at AJA University of Medical Sciences approved all of the animal procedures in this research (6.5.201897000577), all animal procedures were performed in accordance with the guidelines for the care and use of laboratory animals. 8-week-old, Wistar rats (male) were used in this study. Each rat was anesthetized with an intraperitoneal injection of ketamine (80 mg/

kg body weight) and xylazine (5 mg/kg). The hairs of the back were shaved and full-thickness wounds (2×2 cm) were created by skin excision. The defects were treated by AME-laden hydrogels (GelMA/AMEs), and cell-laden hydrogels (GelMA/AMEs/ucMSCs) for 21 days. The wounds in the control group were untreated. Sterile Vaseline gauze was used as a secondary dressing. The secondary dressing was changed every 3 days, the wound was cleaned with saline (0.9 wt.%). All animals received tramadol hydrochloride (3 mg/kg) and gentamicin (15 mg/kg) for 3 days postoperative. The health condition was monitored by a veterinarian. Animals were allowed to move freely in their cages and were fed a standard laboratory diet. The progress of healing was recorded by photograph on days 0, 7, 14, and 21. The rats were sacrificed after 3 weeks. For histological evaluation of healed skin, dissected samples were washed in PBS to remove blood and further fixed in formalin (10 wt.%) for two days and then immersed in paraformaldehyde (4 wt.%) at 4 °C. Subsequently, the tissues were embedded in paraffin, slide was stained with hematoxylin and eosin (H&E) and Masson Trichrome (MT). Finally, they were examined under a light microscope (Olympus BX51).

Histological studies

To stain the tissue sections for Immunohistochemistry, the sections were first deparaffinized in xylene, rehydrated via EtOH gradients, and then treated with an antigen retrieval solution containing sodium citrate buffer (pH 6), at a temperature of 90 °C, for 30 min. The sections were then blocked with 10% goat serum (v/v). Primary antibodies for CD31 were stained with Abcam (ab34712) (1:200 dilution), followed by secondary antibodies for IgG (Invitrogen (A11001, A11008, 1:500 dilution).

Statistical analysis

All experiments were repeated at least 3 times and results were expressed as Mean ± SD. Kruskal Wallis Rank Sum Test was used (an alternative to the non-parametric version ANOVA test) to compare the median of outcomes across groups. After a statistically significant Kruskal Wallis test, Dunn's test was used for several pairwise comparisons, and adjusted P-values were used to account for multiple tests (Bonferroni approach) and $P<0.05$ was considered statistically significant across all statistical tests. All analyses were performed with R Statistical Software (R Core Team 2022 Version 4.2.2).

Results

Characterization of Gelatin methacrylate (GelMA) and prepared hydrogels

Fourier transform infrared spectrometer analysis

As shown in FTIR data, the GelMA (SAM-loaded) showed clear peak changes from NpGel approximately 3000 cm^{-1} (Figure 2A). The amide B band was observed at 3078 cm^{-1} (37), indicating that MA and gelatin were successfully cross-linked through the formation of an amide bond. The FTIR data demonstrated that, although physically combined, GelMA and SAM may also create amide bonds by photo-crosslinking. This unique structure cannot be broken apart without disintegrating covalent connections, distinguishing it from interpenetrating networks that comprise two or more distinct networks (38). It was demonstrated by the mechanical characteristics test that GelMA created a sturdy structure.

Analysis of the mechanical properties of hydrogels

The compressive modulus rate in NpGel and GelMA hydrogels was 2 kPa and 26 kPa, respectively (Figure 2B). Since
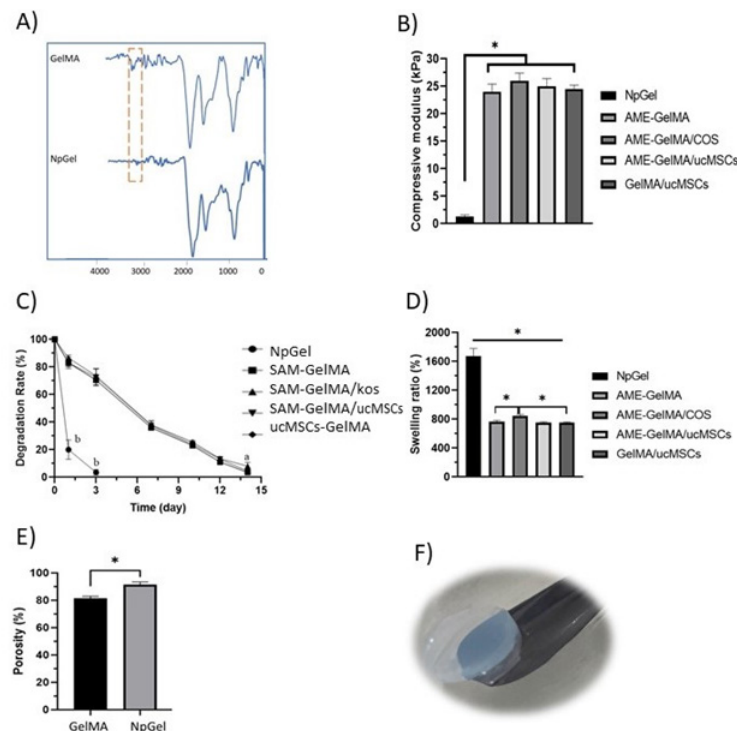
Figure 2. Synthesis and Physical characterization of gelatin methacrylate hydrogels (GelMA)

A) Fourier transform infrared spectrometer analysis of GelMA. B) Compressive modulus of hydrogels; *<0.05. C) Degradation behavior of the hydrogels during 14 days in DMEM/F12 medium containing (100 μg/ml collagenase enzyme) a: *P<0.05*, b: *P<0.01*. C) GelMA hydrogel. D) Swelling profile during 24 hr; *<0.05. E) Porosity of hydrogels (*<0.05(. F) GelMA hydrogel. NpGel; Non-photo-crosslinking Gelatin, SAM-GelMA; Soluble amniotic membrane loaded in gelatin methacrylates, SAM-GelMA/KOS; Soluble amniotic membrane loaded in gelatin methacrylate conjugate by keratose, SAM-GelMA/uuMSCs; Soluble amniotic membrane loaded in gelatin methacrylate contain umbilical cord mesenchymal stem cell

the NpGel hydrogel has only physical crosslinks, it showed a low compressive modulus, which was expected. However, GelMA hydrogel showed a higher compressive modulus, which prevents its contraction in the culture medium.

Degradation profile of hydrogels

The stability of hydrogels was evaluated by degradation assay during 7 days in the enzyme solution. Collagenase enzyme is a protease that consists of a polypeptide chain and is capable of digesting collagen fibers (36). Gelatin covalent bonds in GelMA hydrogel can reduce the rate of biodegradation in the presence of collagenase. Due to the absence of chemical bonds, NpGel hydrogel showed faster degradation in comparison with GelMA hydrogel. The weight loss of NpGel hydrogel ($81.8\pm2.1\%$) on the first day in comparison with the GelMA sample ($13.7\pm1.9\%$) indicated the greater stability of chemically crosslinked gelatin against enzymatic degradation. Figure 2C shows that the gelatin hydrogel is completely degraded within 3 days in the enzyme solution, while the remaining weight of GelMA was calculated ($63.7\pm1.3\%$).

Swelling behavior and porosity of hydrogel

The swelling rate of NpGel physical hydrogel ($868.3\pm25.1\%$) indicated a significant increase in comparison with GelMA chemical hydrogel ($730.8\pm20.3\%$) (Figure 2D). Indeed, GelMA swelling reduction was attributed to the tough structure resulting in chemical bonds between the methacryloyl gelatin chains. Furthermore, methacryloyl bonds, which have little hydrophilicity, replace the hydrophilic amine functional group in the polymer chain (39). Furthermore, gelatin hydrogel water absorption increased porosity and open network structure of hydrogel. In contrast, increasing the density of gelatin crosslinking resulted in the formation of smaller pores throughout

the GelMA hydrogel. Since porosity is necessary for cell migration and nutrient exchange, the porosity of hydrogels was measured by the liquid displacement method. The porosity rate was calculated in NpGel ($93.5\pm1.3\%$) and GelMA hydrogel ($24.8\pm1.5\%$) (Figure 2E). These results showed that the porosity range of hydrogels is suitable for maintaining cell migration, proliferation, and nutrient exchange.

*Determination of crosslinked component of GelMA*

The relative degree of crosslinking of the hydrogel after methacrylate was assessed by Acid-soluble gel. It should be minimal when all the free groups of gelatins are crosslinked together except for extractable gelatins. As shown in Figure 3A, all the remaining GelMA mass was $68.2\pm2.21\%$ after a 3-time soak in HCL solution, while the non-crosslinked sample was $10.25\pm0.14\%$. These results showed that photo-crosslink of modified gelatin was successful and most gelatin chains participated in this reaction, further supporting FTIR information.

Analysis of the SAM protein from hydrogel in vitro

The *in vitro* release of EGF from SAM-GelMA, SAM-GelMA/COS, and NpGel groups was assessed for 14 days. As shown in Figure 3B, there was significantly less cumulative release of EGF from the SAM-GelMA/KOS ($22\pm0.7\%$) hydrogel in comparison with the SAM-GelMA hydrogel ($41.5\pm0.4\%$) in day 1. Also, there was significantly less cumulative release of EGF from the SAM-GelMA group compared with the NpGel.

Optimization of the SAM dosage

Metabolic activity of MSCs-laden SAM-loaded hydrogels was assessed by MTS assay on days 1 and 7 (Figure 4a). All samples revealed good cytocompatibility during 7 days; each group had significant increases in OD from Day 3 to Day
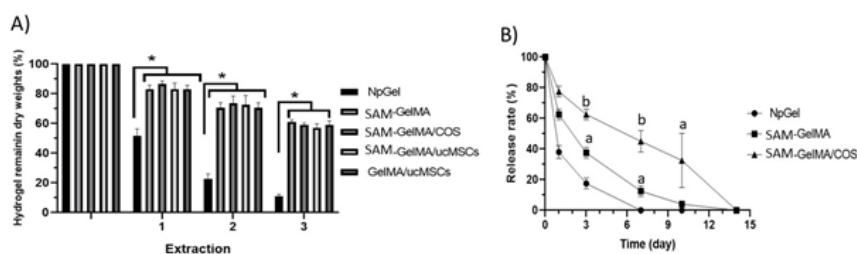

Figure 3. Release behavior of epidermal growth factors
A) Determination of chemical modification of photo-crosslinkable GelMA; *<0.05. (B) Cumulative EGF release from hydrogels over 14 days (a, b). Significant difference between SAM-GelMA/KOS and the other groups; a: *P*<0.05, b: *P*<0.01); kOS, Kerateose
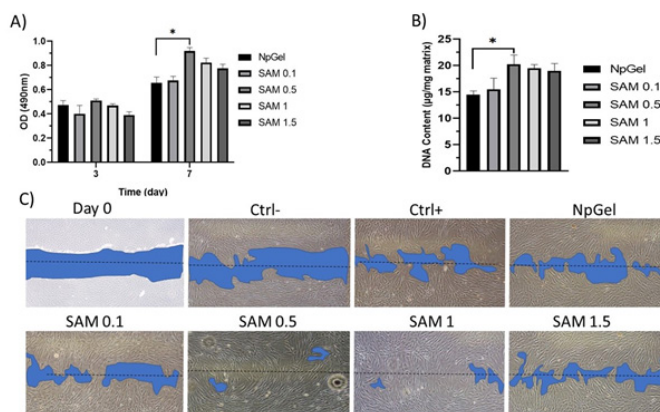
Figure 4. Cytocompatibility of cell-laden hydrogels
(A) MTS assay of the Mesenchymal stem cells/Solubilized AM (MSC/SAM) encapsulated in the hydrogels at different time points. A significant difference between the optical density [OD] of SAM 0.5 compared with NpGel-MSCs (without SAM); *<0.05. (B) Quantification of DNA content within 7 days from cell culture; *<0.05. (C) Microscopic images from HDFs morphology treated with different CM and control groups; Ctrl -: conditioned medium (CM) free DMEM, Ctrl +: FBS/DMEM, SAM 0.1:CM prepared from SAM 0.1 mg/ml, and MSCs (1×10^5 cell/ml) loaded in the hydrogel; HDFs: human dermal fibroblast
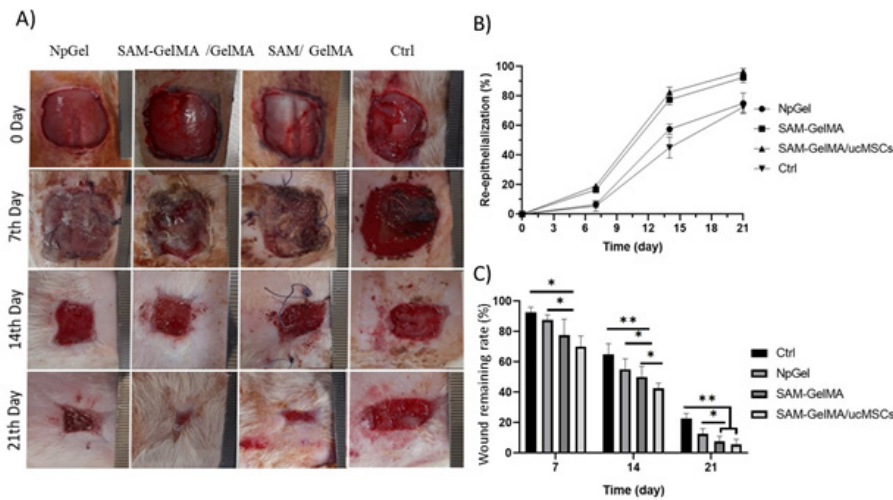
Figure 5. Macroscopic images of rat wound healing
A) Digital images were provided after the 3rd, 7th, 14th, and 21st day of injury. B). Wound remaining (%) was calculated by dividing the remaining wound surface by the surface of the original wound size. The GelMA group accelerated wound closure C): Re-epithelialization of the wound was calculated by measuring the residual wound area and contraction by measuring the new epithelialization skin of the wound; * <0.05, ** < 0.01.

7. Interestingly, the OD in MSCs-laden hydrogels loaded with SAM (0.5 mg/ml) significantly increased on day 7 compared with the control group (0.92±0.08 vs 0.65±0.04). Quantification of DNA content within 7 days from cell seeding has been used to assess *in vitro* proliferation. As shown in Figure 4B, the DNA content of MSCs-laden hydrogels loaded with SAM (0.5 mg/ml) group significantly increased compared with the other hydrogel (21.2±1.5 vs 13.8±1.4 µg/ml matrix). Conditioned medium prepared from cell-laden SAM-loaded hydrogel was assessed in in vitro migration assay during 12 hr (Figure 4C). According to the microscopic images of the scratch area, cell migration was observed after 3 hr in all groups. The scratch area in the wells treated with SAM (0.5 mg/ml) group (95±3.1%) was decreased compared with positive Ctrl (65±2.7%) and NpGel (67.1±2.4%) groups after 12 hr.

Wound morphology and hydrogel scaffold fate
GelMA hydrogels were observed for 10 days at the wound site. Then they were replaced with new dermal and epithelial tissue. Gelatin hydrogel was seen on the wound during 6 days, and in the control group scab tissue was observed at the control (without treatment) wound site (Figure 5A).

Re-epithelialization
The rate of epithelial tissue formation of the healed skin is defined as a percentage in each time period. As shown in Figure 5B, there was no significant difference between different groups during the 3 days, but the formation of epithelial tissue in the SAM-GelMA/ucMSCs group on days 7, 14, and 21 showed a significant increase compared to other groups. The epithelial tissue on day 7 was much higher in the SAM-GelMA group (44.7 ± 0.79%) compared to the control group (26.6 ± 0.12%). The epithelialization in the SAM-GelMA/ucMSCs group (77.8±1.13%) and SAM-GelMA (69.3±0.97%) showed a significant increase compared to the control group (51.6 ± 1.18%) on day 14.

Wound healing rate
Wound area reduction in the SAM-GelMA and SAM-GelMA/ucMSCs groups was significantly higher compared with the positive control group (NpGel) and negative control (Figure 5C), the progress of wound healing was

obvious after 7 days. Wound remaining in the SAM-GelMA/ucMSCs group (3.2±0.21%) was less than other control groups (25.1±1.31%), SAM-GelMA (8.2 ± 1.25%).

Histological studies
Wound healing is a temporary process that requires the coordinated activity of many factors such as growth factors and cytokines, extracellular matrix, blood vessels, and different types of cells (8). In order to evaluate the infrastructure of skin and wound healed with SAM-GelMA and SAM-GelMA/ucMSCs groups, H&E staining was performed. The surface area of the wound was evaluated by collecting a series of individual images using ImageJ software in one image (Figure 6A). This evaluation shows that the thickness of the new skin in the control group is thinner than in the treatment groups (Figure 6B). The appearance of hair in the repaired skin and tissue appendages such as hair follicles and sweat glands was observed in the central area of the wound, which was attributed to the migration and proliferation of endogenous cells. Infiltration of macrophages was observed in all groups on day 3. While, in SAM-GelMA and SAM-GelMA/MSCs due to the strong anti-inflammatory activity of SAM, less inflammation was observed than in the control group. In addition, angiogenesis was observed in the granulation tissue and in SAM-GelMA and SAM-GelMA/MSCs, which can be attributed to the presence of SAM and angiogenesis-stimulating growth factors such as VEGF. As reported, the presence of blood vessels is necessary for granulation tissue formation, because it carries out oxygenation, nutrition, and removal of waste materials. Fibroblast infiltration and neovascularization increased on days 7 and 14, and wound healing appeared. In the study of MT staining, it was observed that the amount of fibrosis in wounds treated with SAM-GelMA and SAM-GelMA/MSCs groups is lower compared to the control group. In addition, the collagen fibers in the SAM-GelMA/MSCs group were organized in a more distinct arrangement, while these fibers were denser and thicker in parallel in the control group.

Angiogenesis
The density of blood vessels was determined by counting the number of blood vessels in different parts of the tissue
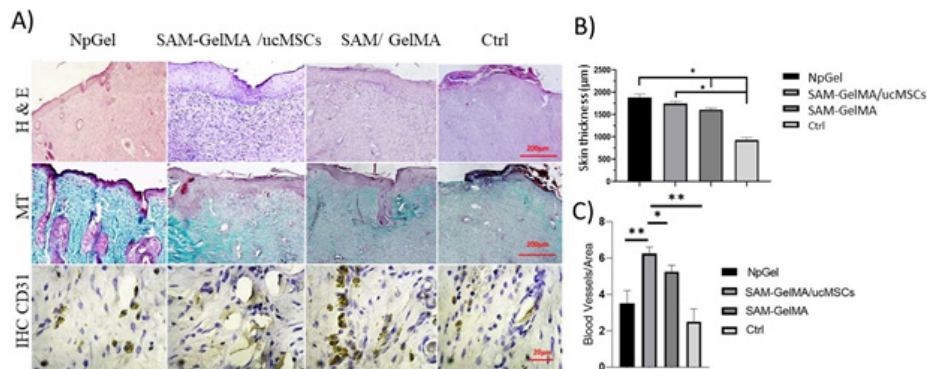
Figure 6. Morphological evaluation of rat skin lesions with histological analysis method
A) H&E and MT staining shows the epidermis and dermis structure. B) Healed skin thickness measures revealed that treated skin, both with SAM-GelMA/ucMSCs and SAM-GelMA, was thicker than untreated wounds. C) Quantification of blood vessel density by counting the number of vessels with high-resolution microscopic images; *<0.05, **<0.01; MT, Masson's trichrome stain; H&E, Hematoxylin and eosin stain.

using high-resolution microscopic images (Figure 6C). The number of blood vessels in the SAM-GelMA/MSCs group (6.3±0.3) was significantly increased compared with the control group (2.2 ± 0.2, Figure 6B).

Discussion

Currently, stem cells and biological sources such as cell secretory (40,41) or tissue-derived structural substances (42) are used to regenerate damaged tissue, further providing an alternative to conventional methods or a successful complementary therapy for wound healing (42). In this regard, researchers developed innovative products that are based on cells (43, 44), cell-derived products such as conditioned media secreted from cell culture loaded in three-dimensional scaffolds (42) and therapeutic properties were evaluated for the fabrication of new skin substitutes. Although previous study indicates that the amnion membrane contains an array of growth factors, proteins, and cytokines (45) that have been shown to promote skin regeneration and wound healing, there is still a major limitation to the delivery and application of this intact amnion to extensive or irregularly shaped wounds (46, 47). This refers to the majority of treatment conditions where an amnion sheet does not adjust an atypical wound size or topology, or where fast degradation because of poor mechanical properties has resulted in the development of a new generation of amnion-derived products (28, 48, 49). The present cell-laden SAM-loaded pre-polymer solution was injected into the wound site, and following exposure to light, it quickly crosslinked to conform toward the wound contour (34). Additionally, its mechanical, degrading, and biological properties may be readily tuned by adjusting the degree of methacrylamide modification, GelMA concentration, or photopolymerization duration (28, 34). Mechanical properties results illustrated that the compression module and degradation rate of cell-laden SAM-loaded GelMA hydrogel significantly increased after photo-crosslinking in comparison with non-photo-crosslinked gelatin hydrogel (Figure 2B). As shown by Zhao et al., higher mechanical properties and slower degradation rates could be obtained at the modification of methacrylamide, GelMA (10 %) 26±3 kPa and 30±2 %, day 3, respectively (34). Our study met the GelMA (10 %) mechanical properties (34). Higher water absorption in NpGel hydrogel led to enhanced porosity and a more open network topology (50). On the other hand, smaller

porosity and higher mechanical properties developed due to increased crosslinking density (39). Fabrication of wound dressing based on gelatin by freeze-drying method revealed higher porosity and mechanical properties (51). The unique characteristics of gelatin are maintained when it is modified with photocrosslinkable methacrylamide groups (GelMA), but the hydrogel additionally exhibits more mechanical properties in comparison with freeze-drying method (51, 52). Crosslinked GelMA kept about 63% of its initial mass whereas the non-cross-linked sample (Figure 5). The crosslinked network was determined using FTIR by integrating peaks that correspond to the aromatic residues of gelatin and double bonds that correspond to methacrylamide. Growth factors loading in the scaffold may be advantageous for regenerating cell-based tissues and could be useful for MSCs support epithelialization (53). It has been demonstrated that sulfated glycosaminoglycan can stabilize keratose-bound growth factors through electrostatic interactions between negatively charged sulfate groups as well as positively charged amino acid residues of growth factors (29,54). The growth factors may be sustained for a long time as a result of this physical binding. SAM has been entrapped in GelMA hydrogels; its release via UV–vis spectroscopy was determined at 278 nm (Figure 3B). The cumulative release of EGF from GelMA hydrogel functionalized by KOS (1 Wt.%) was significantly lower in comparison to that of GelMA and gelatin hydrogels. Since the chemical structures of the SAM and GelMA hydrogel both include an aromatic segment, the EGF could be bound non-covalently to the GelMA-KOS. As a result, GelMA/KOS hydrogel may sustain SAM release with variable molecule sizes more effectively than KOS-free GelMA (Figure 3B). According to Momeny et al., 34.5% of the total SAM protein release occurred within the first 48 hr (19), but Murphy et al. observed that SAM protein bulk release occurred within the first week (20). SAM-GelMA/KOS additionally reduced the cumulative release of the SAM proteins. Our previous study (45) indicated that Amniotic membrane Extract (AME) prepared by sonication method, concentration of 1 mg/ml, significantly increased fibroblast proliferation and migration which aligned with the results reported by Momeny *et al.* (19). While, in the current study, the concentration of 0.5 mg/ml increases the proliferation and migration of fibroblast and MSCs loaded in the hydrogel. The OD of NpGel loaded with only MSCs revealed a considerable increase on day 3. On day 7, it showed a significant decrease when compared

to the group that had cell-laden GelMA/SAM 0.5 mg/ml. The result can be attributed to the hydrogel scaffold contracting and cell death caused by the accumulation of cells (42). Human dermal fibroblast (HDF) migration is greatly increased by condition medium generated by MSCs-laden SAM-loaded hydrogel when compared to another group. This is supported by the paracrine activity of SAM and MSCs, which is consistent with the research conducted (55) to assess the effect of AME on cell ucMSCs culture (55). According to a study's results, ucMSCs conditioned medium was migrating HDF (56). We demonstrated that both the SAM-loaded GelMA and SAM-loaded GelMA hydrogels with encapsulated MSCs could facilitate the repair of rat skin defects, which was presumably due to prolonged release and better retention of SAM and cytokine released from ucMSCs. The morphological analysis of the cell-laden SAM-loaded GelMA hydrogel group greatly increased the percentage of wound closure by re-epithelialization and reducing wound contraction. In the histology evaluations, the GelMA group contained cells and SAM revealed thicker healed skin and more neovascularization generally (57). Fibroblast growth factor (FGF-family), epidermal growth factor receptor (EGF-R), epidermal growth factor (EGF), and vascular endothelial growth factor (VEGF), all of which are involved in the formation of new blood vessels, were significantly increased in the cell-laden SAM-loaded GelMA group compared to other groups (58, 59). Indeed, this study supports the effects of GelMA on survival, fibroblast activity, and prevention of wound contraction as well as the effect of SAM and MSCs together to boost growth factors that are useful in wound healing. The cell-laden SAM-loaded GelMA hydrogel supports the proliferation and migration of fibroblasts in in vitro and in vivo conditions. The rat full-thickness wound model and its repair are commonly used in basic research to evaluate potential therapies for wound repair. However, there are major limitations to these models that are well known, such as not being similar to humans, endogenous repair of rats, and wound repair without any therapeutic measures. However, on days 3, 7, 14, and 21 in this study, we compared the effect of epithelialization, contraction, and percentage of wound healing in the groups. Considering that we found that there are significant changes in these parameters, we predict that this improvement will be much more effective in chronic wounds and wounds that have a slow healing process. Also, it is difficult to evaluate the long-term scar due to the rapid closure of the wound in the healthy rats used in this study.

Conclusion

This study was designed in order to fabricate and evaluate the in situ SAM-loaded cell-laden hydrogel with the controlled drug release ability for the regeneration of full-thickness skin defects in rats. According to the results, the mechanical properties of the photo-crosslinkable hydrogel, degradation in the presence of collagenase enzyme (13.7 ± 1.9%), and compression module (26 kPa), were increased. In this regard, conjugation of a methacrylate functional group onto the hydroxyl or amine groups of gelatin was confirmed by Fourier transform infrared (FTIR) spectroscopy at a resolution of 3078 cm^{-1}. The viability and proliferation of ucMSCs loaded in the photo-crosslinkable hydrogel were increased in the presence of the SAM (0.5 mg/ml) during 7 days after culture. We demonstrated that incorporation of keratos (1%) with high affinities to biological agents could stabilize and improve the sustained release of SAM

(22±0.7%). CM prepared from hydrogels containing SAM and MSCs can increase the migration of fibroblasts in in vitro conditions. In this regard, SAM (0.5 mg/ml) revealed the greatest effect on migration of fibroblasts compared to other concentrations of SAM (0.1,1 and 1.5 mg/ml). GelMA scaffold prevented wound contraction, and the simultaneous presence of SAM and ucMSCs increases the rate of healing, angiogenesis, and wound closure. This in situ hydrogel can be used as a new skin substitute for rapid wound repair and regeneration and further studies in the clinical environment.

Authors' Contributions

M AA and Z J conceived, designed, and conducted the experiment. M AA wrote the manuscript. A E re-analyzed the statistical data and results. MA H re-analyzed the data and edited the manuscript.

Conflicts of Interest

No declarations of interest are reported by the authors.

References

1. Shukla SK, Sharma AK, Gupta V, Yashavarddhan MH. Pharmacological control of inflammation in wound healing. J Tissue Viability 2019; 28: 218-222.
2. Geanaliu-Nicolae RE, Andronescu E. Blended natural support materials—collagen based hydrogels used in biomedicine. Mater (Basel) 2020;13:1–31.
3. Sorg H, Tilkorn DJ, Hager S, Hauser J, Mirastschijski U. Skin wound healing: An update on the current knowledge and concepts. Eur Surg Res 2017;58:81–94.
4. Stamm A, Reimers K, Strauß S, Vogt P, Scheper T, Pepelanova I. *In vitro* wound healing assays–state of the art. BioNanoMat 2016;17:79-87.
5. Zheng Y, Zheng S, Fan X, Li L, Xiao Y, Luo P, *et al*. Amniotic epithelial cells accelerate diabetic wound healing by modulating inflammation and promoting neovascularization. Stem Cells Int 2018; 25: 142-187.
6. Gushiken LF, Beserra FP, Bastos JK, Jackson CJ, Pellizzon CH. Cutaneous wound healing: An update from physiopathology to current therapies. Life 2021; 11: 665-679.
7. Wilkinson HN, Hardman MJ. Wound healing: Cellular mechanisms and pathological outcomes. Open Biol 2020; 10: 200223.
8. Eming SA, Martin P, Tomic-Canic M. Wound repair and regeneration: mechanisms, signaling, and translation. Sci Transl Med 2014; 265: p.265sr6-265sr6.
9. Lipsky BA, Aragón-Sánchez J, Diggle M, Embil J, Kono S, Lavery L, *et al*. IWGDF guidance on the diagnosis and management of foot infections in persons with diabetes. Diabetes Metab Res Rev 2016; 32: 45–74.
10. Boateng J, Catanzano O. Advanced therapeutic dressings for effective wound healing - a review. J Pharm Sci 2015;104: 3653–3680.

11. Goula A, Gkioka V, Michalopoulos E, Katsimpoulas M, Noutsias M, Sarri EF, *et al*. Advanced therapy medicinal products challenges and perspectives in regenerative medicine. J Clin Med Res 2020;12:780–786.

12. Balasubramani V, Jeganathan R, Kumar SD. Numerical analysis of porosity effects on mechanical properties for tissue engineering scaffold. Mater Today Proc 2023; 30:124.

13. Park JW, Hwang SR, Yoon IS. Advanced growth factor delivery systems in wound management and skin regeneration. Molecules 2017; 22.8: 1259

14. Koizumi N, Inatomi T, Sotozono C, Fullwood NJ, Quantock AJ, Kinoshita S. Growth factor mRNA and protein in preserved human amniotic membrane. Curr Eye Res 2000; 20:173–177.

15. Murphy SV, Skardal A, Song L, Sutton K, Haug R, Mack DL, *et al*. Solubilized amnion membrane hyaluronic acid hydrogel accelerates full-thickness wound healing. Stem Cells Transl Med 2017; 6: 2020–2032.

16. Murri MS, Moshirfar M, Birdsong OC, Ronquillo YC, Ding Y, Hoopes PC. Amniotic membrane extract and eye drops: A review of literature and clinical application. Clin Ophthalmol 2018;12:1105–1112.

17. Elkhenany H, El-Derby A, Abd Elkodous M, Salah RA, Lotfy A, El-Badri N. Applications of the amniotic membrane in tissue engineering and regeneration: the hundred-year challenge. Stem Cell Res Ther 2022;13:1-9.

18. Asl NS, Nejat F, Mohammadi P, Nekoukar A, Hesam S, Ebrahimi M, *et al*. Amniotic membrane extract eye drop promotes limbal stem cell proliferation and corneal epithelium healing. Cell J 2019; 20: 459–468.

19. Momeni, Maryam, *et al*. *In vitro* and *in vivo* investigation of a novel amniotic-based chitosan dressing for wound healing. Wound Repair Regen 2018; 26: 87–101.

20. Bhattacharjee M, Escobar Ivirico JL, Kan HM, Shah S, Otsuka T, Bordett R, *et al*. Injectable amnion hydrogel-mediated delivery of adipose-derived stem cells for osteoarthritis treatment. Proc Natl Acad Sci U S A 2022; 119:e2120968119.

21. Bayat S, Zabihi AR, Farzad SA, Movaffagh J, Hashemi E, Arabzadeh S, *et al*. Evaluation of debridement effects of bromelain-loaded sodium alginate nanoparticles incorporated into chitosan hydrogel in animal models. Iran J Basic Med Sci 2021; 24:1404–1412.

22. Soheilifar MH, Masoudi-Khoram N. Wound dressings incorporating microRNAs: Innovative therapy for diabetic wound treatment. Iran J Basic Med Sci 2022; 26:1042–1044.

23. Samadian H, Vahidi R, Salehi M, Hosseini-Nave H, Shahabi A, Zanganeh S, *et al*. Hydrogel nanocomposite based on alginate/zeolite for burn wound healing: *In vitro* and *in vivo* study. Iran J Basic Med Sci 2023; 26:708–716.

24. Shin H, Olsen BD, Khademhosseini A. The mechanical properties and cytotoxicity of cell-laden double-network hydrogels based on photocrosslinkable gelatin and gellan gum biomacromolecules. Biomater 2012; 33:3143–3152.

25. Xiao S, Zhao T, Wang J, Wang C, Du J, Ying L, *et al*. Gelatin methacrylate (GelMA)-based hydrogels for cell transplantation: an effective strategy for tissue engineering. Stem Cell Rev Rep 2019;15: 664–679.

26. Nguyen AH, McKinney J, Miller T, Bongiorno T, McDevitt TC. Gelatin methacrylate microspheres for controlled growth factor release. Acta Biomater 2015; 13:101–110.

27. Öztürk E, Arlov Ø, Aksel S, Li L, Ornitz DM, Skjåk-Bræk G, Zenobi-Wong M. Sulfated hydrogel matrices direct mitogenicity and maintenance of chondrocyte phenotype through activation of FGF signaling. Adv Funct Mater. 2016; 26: 3649-3662.

28. Zhang Q, Chang C, Qian C, Xiao W, Zhu H, Guo J, *et al*. Photo-crosslinkable amniotic membrane hydrogel for skin defect healing. Acta Biomater 2021; 125:197–207.

29. Ledford B, Barron C, Van Dyke M, He JQ. Keratose hydrogel for tissue regeneration and drug delivery. Semin Cell Dev Biol

2022; 128:145–153.

30. Song Y, Nagai N, Saijo S, Kaji H, Nishizawa M, Abe T. In situ formation of injectable chitosan-gelatin hydrogels through double crosslinking for sustained intraocular drug delivery. Mater Sci Eng C Mater Biol Appl 2018; 88:1–12.

31. Keriquel V, Guillemot F, Arnault I, Guillotin B, Miraux S, Amédée J, *et al*. *In vivo* bioprinting for computer-and robotic-assisted medical intervention: preliminary study in mice. Biofabrication 2010; 2:014101.

32. Hong IS. Enhancing stem cell-based therapeutic potential by combining various bioengineering technologies. Front Cell Dev Biol 2022; 10: 901661.

33. Luo G, Cheng W, He W, Wang X, Tan J, Fitzgerald M, *et al*. Promotion of cutaneous wound healing by local application of mesenchymal stem cells derived from human umbilical cord blood. Wound Repair Regen 2010; 18: 506–513.

34. Zhao X, Lang Q, Yildirimer L, Lin ZY, Cui W, Annabi N, *et al*. Photocrosslinkable gelatin hydrogel for epidermal tissue engineering. Adv Healthc Mater 2016; 5: 108–118.

35. Brinkman WT, Nagapudi K, Thomas BS, Chaikof EL. Photo-cross-linking of type I collagen gels in the presence of smooth muscle cells: Mechanical properties, cell viability, and function. Int J Biol Macromol 2003; 4: 890–895.

36. Ågren MS, Taplin CJ, Woessner JF, Eaglstein WH, Mertz PM. Collagenase in wound healing: Effect of wound age and type. J Invest Dermatol 1992; 99: 709–714.

37. Zhou X, Zhu W, Nowicki M, Miao S, Cui H, Holmes B, *et al*. 3D bioprinting a cell-laden bone matrix for breast cancer metastasis study. ACS Appl Mater Interfaces 2016; 8:30017–30026.

38. Fonseca DFS, Costa PC, Almeida IF, Dias-Pereira P, Correia-Sá I, Bastos V, *et al*. Swellable gelatin methacryloyl microneedles for extraction of interstitial skin fluid toward minimally invasive monitoring of urea. Macromol Biosci 2020; 20:2000195.

39. Baei P, Daemi H, Mostafaei F, Azam Sayahpour F, Baharvand H, Baghaban Eslaminejad M. A tough polysaccharide-based cell-laden double-network hydrogel promotes articular cartilage tissue regeneration in rabbits. Chem Eng J 2021; 418:129277.

40. Kim MH, Wu WH, Choi JH, Kim JH, Hong SH, Jun JH, *et al*. Conditioned medium from the three-dimensional culture of human umbilical cord perivascular cells accelerate the migration and proliferation of human keratinocyte and fibroblast. J Biomater Sci Polym Ed 2018; 29:1066–1080.

41. Hur W, Lee HY, Min HS, Wufuer M, Lee C won, Hur JA, *et al*. Regeneration of full-thickness skin defects by differentiated adipose-derived stem cells into fibroblast-like cells by fibroblast-conditioned medium. Stem Cell Res Ther 2017; 8:1-3.

42. Maarof M, Mh Busra MF, Lokanathan Y, Bt Hj Idrus R, Rajab NF, Chowdhury SR. Safety and efficacy of dermal fibroblast conditioned medium (DFCM) fortified collagen hydrogel as acellular 3D skin patch. Drug Deliv Transl Res 2019; 9: 144–161.

43. Armstrong DG. The efficacy of Apligraf in the treatment of diabetic foot ulcers. Plast Reconstr Surg 2006;117:152S-157S.

44. Marston WA. Dermagraft®, a bioengineered human dermal equivalent for the treatment of chronic nonhealing diabetic foot ulcer. Expert Rev Med Devices 2004; 1:21–31.

45. Alamouty MA, Asl NS, Safari A, Ebrahimi M, Daemi H. Fabrication of cell-laden AME-loaded collagen-based hydrogel promotes fibroblast proliferation and wound healing *in vitro*. Cell J 2023; 25:255–263.

46. Tehrani FA, Ahmadiani A, Niknejad H. The effects of preservation procedures on antibacterial property of amniotic membrane. Cryobiology 2013; 67:293–298.

47. Haugh AM, Witt JG, Hauch A, Darden M, Parker G, Ellsworth WA, *et al*. Amnion membrane in diabetic foot wounds: A meta-analysis. Plast Reconstr Surg - Glob Open 2017; 5:e1302.

48. Chopra, Aditi, and Betsy S. Thomas. Amniotic membrane: A novel material for regeneration and repair. J Biomim Biomater

Tissue Eng 18.1: 2013; 1-8.

49. Taghiabadi E, Nasri S, Shafieyan S, Firoozinezhad SJ, Aghdami N. Fabrication and characterization of spongy denuded amniotic membrane based scaffold for tissue engineering. Cell J 2015;16:476–487.

50. Heydary HA, Karamian E, Poorazizi E, Khandan A, Heydaripour J. A novel nano-fiber of iranian gum tragacanth-polyvinyl alcohol/nanoclay composite for wound healing applications. Procedia Mater Sci 2015; 11:176–182.

51. Doozandeh Z, Saber-Samandari S, Khandan A. Preparation of novel arabic gum-c6h9no biopolymer as a bedsore for wound care application. Acta Med Iran 2020; 58:520–530.

52. Karimi M, Asefnejad A, Aflaki D, Surendar A, Baharifar H, Saber-Samandari S, *et al.* Fabrication of shapeless scaffolds reinforced with baghdadite-magnetite nanoparticles using a 3D printer and freeze-drying technique. J Mater Res Technol 2021;14: 3070–3079.

53. Stanton AE, Tong X, Yang F. Extracellular matrix type modulates mechanotransduction of stem cells. Acta Biomater 2019; 96: 310–320.

54. de Guzman RC, Saul JM, Ellenburg MD, Merrill MR, Coan HB, Smith TL, *et al.* Bone regeneration with BMP-2 delivered from

keratose scaffolds. Biomaterials 2013; 34:1644–1656.

55. Vojdani Z, Babaei A, Vasaghi A, Habibagahi M, Talaei-Khozani T. The effect of amniotic membrane extract on umbilical cord blood mesenchymal stem cell expansion: Is there any need to save the amniotic membrane besides the umbilical cord blood? Iran J Basic Med Sci 2016; 19: 89–96.

56. Arno AI, Amini-Nik S, Blit PH, Al-Shehab M, Belo C, Herer E, Tien CH, *et al.* Human Wharton's jelly mesenchymal stem cells promote skin wound healing through paracrine signaling. Stem Cell Res Ther 2014; 5: 1–13.

57. Dinh T, Braunagel S, Rosenblum BI. Growth Factors in Wound Healing: The present and the future?." Clin Podiatr Med Surg 2015; 32.1: 109-119.

58. Rustad KC, Wong VW, Sorkin M, Glotzbach JP, Major MR, Rajadas J, *et al.* Enhancement of mesenchymal stem cell angiogenic capacity and stemness by a biomimetic hydrogel scaffold. Biomaterials 2012; 33:80–90.

59. Yu A, Matsuda Y, Takeda A, Uchinuma E, Kuroyanagi Y. Effect of EGF and bFGF on fibroblast proliferation and angiogenic cytokine production from cultured dermal substitutes. J Biomater Sci Polym Ed 2012; 23: 1315–1324.